

# Axially Chiral Directly $\beta,\beta$ -Linked Bisporphyrins: Synthesis and Stereostructure

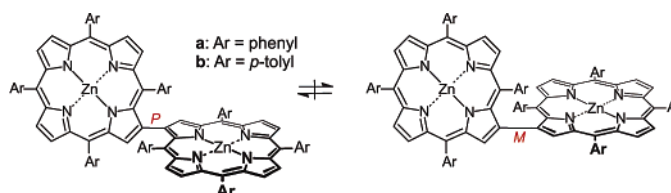
Gerhard Bringmann,\* Stefan Rüdener, Daniel C. G. Götz,  
Tobias A. M. Gulder, and Matthias Reichert

Institute of Organic Chemistry, University of Würzburg, Am Hubland,  
D-97074 Würzburg, Germany

bringman@chemie.uni-wuerzburg.de

Received July 22, 2006

## ABSTRACT



A novel type of “superbiaryl”, the first porphyrin dimers with an intrinsically chiral structure, has been prepared. The atropo-enantiomers were configurationally assigned by HPLC–CD combined with quantum chemical CD calculations.

Axially chiral biaryl systems are of increasing importance as bioactive natural products<sup>1</sup> but also as efficient reagents and as ligands for asymmetric synthesis.<sup>2–4</sup> An attractive extension of this class of compounds might be expected from rotationally hindered bisporphyrins because they should combine the useful properties of axial chirality and porphyrin chemistry and thus could open new perspectives in the development of novel chiral catalysts, reagents, optical and electronic devices, chiral reporter groups, or novel materials with pronounced chiral and chiroptical properties.

Besides monomeric porphyrins that owe their axial chirality to rotationally hindered *meso*-aryl substituents,<sup>5</sup> molecules have been reported in which two porphyrin entities are linked via a chiral central biaryl core.<sup>2–9</sup> Recently, Osuka et al. have

described the design, synthesis, and stereochemical properties of directly *meso–meso* and *meso- $\beta$* -linked porphyrin dimers.<sup>10–13</sup> The axial chirality of their singly linked examples, however, does not result from the parent bisporphyrin framework itself (which, as such, has a plane of symmetry and is thus achiral) but only from the unsymmetric pattern of their remote *meso*-substituents. Of particular interest would thus be the design and synthesis of directly  $\beta,\beta$ -coupled bisporphyrins, which, due to the more peripheral position of the heterobiaryl axis, are already axially chiral per se, independent from their substituents, and should, in addition, open a vast, stereochemically largely differentiated chiral cavity. Still, none of the few representatives prepared

(1) Bringmann, G.; Price Mortimer, A. J.; Keller, P. A.; Gresser, M. J.; Garner, J.; Breuning, M. *Angew. Chem., Int. Ed.* **2005**, *44*, 5518.

(2) Bringmann, G.; Breuning, M. *Tetrahedron: Asymmetry* **1998**, *9*, 667.

(3) Bringmann, G.; Pfeifer, R. M.; Rummey, C.; Hartner, K.; Breuning, M. *J. Org. Chem.* **2003**, *68*, 6859.

(4) Bringmann, G.; Pfeifer, R. M.; Schreiber, P.; Hartner, K.; Schraut, M.; Breuning, M. *Tetrahedron* **2004**, *60*, 4349.

(5) Medforth, C. J.; Haddad, R. E.; Muzzi, C. M.; Dooley, N. R.; Jaquinod, L.; Shyr, D. C.; Nurco, D. J.; Olmstead, M. M.; Smith, K. M.; Ma, J.-G.; Shelnutt, J. A. *Inorg. Chem.* **2003**, *42*, 2227.

(6) Hayashi, T.; Aya, T.; Nonoguchi, M.; Mizutani, T.; Hisaeda, Y.; Kitagawa, S.; Ogoshi, H. *Tetrahedron* **2002**, *58*, 2803.

(7) Hayashi, T.; Nonoguchi, M.; Aya, T.; Ogoshi, H. *Tetrahedron Lett.* **1997**, *38*, 1603.

(8) Naruta, Y.; Ishihara, N.; Tani, F.; Maruyama, K. *Bull. Chem. Soc. Jpn.* **1993**, *66*, 158.

(9) Zaoying, L.; Jianglin, L.; Cong, L.; Wei, X. *Synth. Commun.* **2000**, *30*, 917.

(10) Kim, D.; Osuka, A. *Acc. Chem. Res.* **2004**, *37*, 735.

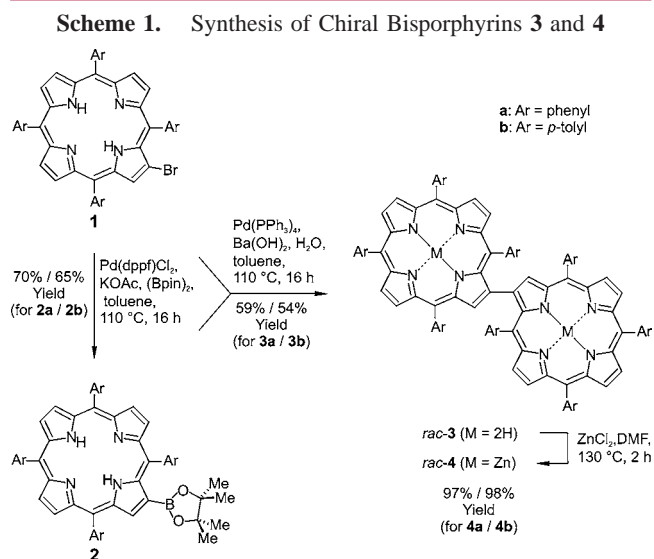
(11) Nakamura, Y.; Hwang, I.-W.; Aratani, N.; Ahn, T. K.; Ko, D. M.; Takagi, A.; Kawai, T.; Matsumoto, T.; Kim, D.; Osuka, A. *J. Am. Chem. Soc.* **2005**, *127*, 236.

(12) Yoshida, N.; Osuka, A. *Tetrahedron Lett.* **2000**, *41*, 9287.

(13) Tsuda, A.; Furuta, H.; Osuka, A. *J. Am. Chem. Soc.* **2001**, *123*, 10304.

so far<sup>14–17</sup> have been recognized as rotationally stable at the porphyrin–porphyrin axis or have even been stereochemically characterized.<sup>18</sup> In this paper, we report on the first intrinsically axially chiral, enantiopure  $\beta,\beta$ -linked porphyrin dimers and their stereochemical characterization by HPLC–CD on a chiral phase and quantum chemical CD calculations.

The synthesis started with the known<sup>19,20</sup> monobromo derivative **1a** of tetraphenylporphyrin (TPP). Attempts to convert **1a** into the new boronic ester **2a** in analogy to conditions described by Deng et al.,<sup>14</sup> however, resulted in the formation of an annulated product (structure not shown).<sup>21</sup> The desired borylation did succeed by applying a procedure by Miyaura,<sup>22</sup> providing **2a** in good yields (Scheme 1). Cross-



coupling of **1a** and **2a** to give the bisporphyrin **3a** was achieved with Pd(PPh<sub>3</sub>)<sub>4</sub> as the catalyst and K<sub>3</sub>PO<sub>4</sub> as a weak base, to avoid hydrodebromination. The initial yield of 26% was increased to 59% by using Ba(OH)<sub>2</sub> in toluene/water.

As expected, the C<sub>2</sub>-symmetric bisporphyrin **3a** displays only one set of signals in <sup>1</sup>H NMR. Depending on the proximity of the four different phenyl groups relative to the central porphyrin–porphyrin axis, these substituents were found to vary largely in <sup>1</sup>H NMR with respect to the chemical

shifts of their protons and their rotational barriers. The most significant effects were those of the protons of the phenyl group at C-5; i.e., the one closest to the central axis and thus also the ones with the most pronounced ring current affected chemical shifts.<sup>23</sup> This phenyl residue showed not only strongly upfield-shifted signals (e.g., the *para*-proton is shifted to 4.70 ppm, compared to the one in TPP<sup>24</sup> resonating at 7.77 ppm) but also, most significantly, a splitting of the corresponding *ortho*- (7.29 and 6.58 instead of 8.22 ppm in TPP<sup>24</sup>) and *meta*-protons (6.22 and 3.87 instead of 7.77 ppm in TPP<sup>24</sup>) into four separate signals, hinting at a restricted rotation about the phenyl–porphyrin axis on the NMR time scale. By high-temperature NMR measurements and application of the Eyring equation, this particular barrier was estimated to be higher than 74 kJ/mol, which is in rough agreement with the calculated value of 86 kJ/mol (AM1<sup>25</sup>).

In contrast to the UV spectrum of monomeric TPP, the Soret band of **3a** is broadened and split due to the exciton coupling between the two porphyrin moieties, in analogy to other  $\beta,\beta$ -coupled bisporphyrins<sup>14</sup> and in perfect accordance with the exciton chirality theory.<sup>26</sup> The B<sub>y</sub> band is slightly blue shifted, and the B<sub>x</sub> band is strongly red shifted. The Q-band absorption is increased in intensity, as compared to the respective bands in TPP (Figure 1).

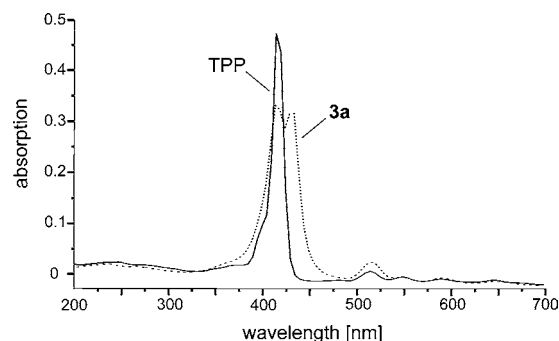


**Figure 1.** UV spectrum of the novel bisporphyrin **3a** as compared to that of its monomeric half, TPP.

Despite numerous attempts on a variety of different chiral HPLC phases, the new bisporphyrin **3a** could not be resolved into its assumed atropo-enantiomers, (*P*)- and (*M*)-**3a**. Its biszinc complex **4a**, by contrast (Scheme 2), gave a good separation on a Chiralcel OD-H column, when decreasing the temperature of the chromatographic system to 7 °C, whereas a separation even at room temperature was attained on a Chirex 3010 column.<sup>27</sup>

(23) A similar behavior was also observed in *meso*- $\beta$ -linked bisporphyrins and corroborated by a crystal structure: Senge, M. O.; Röbber, B.; von Gersdorff, J.; Schäfer, A.; Kurreck, H. *Tetrahedron Lett.* **2004**, *45*, 3363.

(24) For comparison, an <sup>1</sup>H NMR spectrum of TPP is available in the Supporting Information.

(25) Dewar, M. J. S.; Zuebisch, E. G.; Healy, E.; Stewart, J. J. P. *J. Am. Chem. Soc.* **1985**, *107*, 3902.

(26) Harada, N.; Nakanishi, K. *Circular Dichroic Spectroscopy: Exciton Coupling in Organic Stereochemistry*; University Science Books: Mill Valley, CA, 1983.

(14) Deng, Y.; Chang, C. K.; Nocera, D. G. *Angew. Chem., Int. Ed.* **2000**, *39*, 1066.

(15) Hata, H.; Shinokubo, H.; Osuka, A. *J. Am. Chem. Soc.* **2005**, *127*, 8264.

(16) Uno, H.; Kitawaki, Y.; Ono, N. *Chem. Commun.* **2002**, 116.

(17) Ikeue, T.; Furukawa, K.; Hata, H.; Aratani, N.; Shinokubo, H.; Kato, T.; Osuka, A. *Angew. Chem., Int. Ed.* **2005**, *44*, 6899.

(18) For a directly  $\beta,\beta$ -linked, yet N-confused, porphyrin dimer that might be axially chiral but has not been stereochemically characterized, see: Chmielewski, P. J. *Angew. Chem., Int. Ed.* **2004**, *43*, 5655.

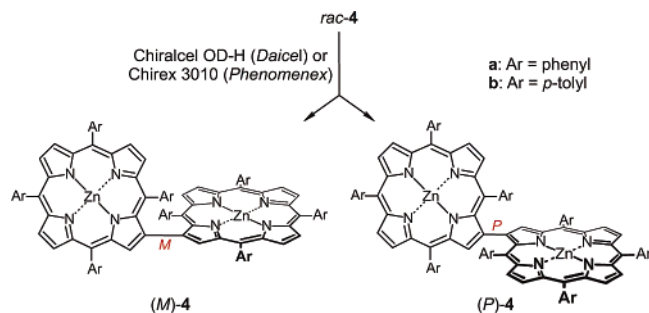
(19) Callot, H. J. *Tetrahedron Lett.* **1973**, *14*, 4987.

(20) Shen, D.-M.; Liu, C.; Chen, Q.-Y. *Chem. Commun.* **2005**, 4982.

(21) When conducting the reaction with Pd(dppf)Cl<sub>2</sub> in DMF as the solvent, the ring-annulated product was obtained in up to 95% yield. During the reviewing process, a similar cyclization reaction was reported, however, with lower yields: Shen, D.-M.; Liu, C.; Chen, Q.-Y. *J. Org. Chem.* **2006**, *71*, 6508.

(22) Ishiyama, T.; Murata, M.; Miyaura, N. *J. Org. Chem.* **1995**, *60*, 7508.

**Scheme 2.** HPLC Resolution of *rac*-**4a,b** into Their Atropo-Enantiomers<sup>28</sup>



That the two resulting LC–UV peaks (Figure 2a) indeed corresponded to the respective atropo-enantiomers of **4a** was demonstrated by their opposite CD effects, as measured online, by LC–CD (Figure 2b), providing a positive CD signal for peak A (“faster”) and a negative one for peak B (“slower”) at 450 nm. For the determination of the absolute configurations of the two atropo-enantiomers, full online CD spectra were recorded in the stopped-flow mode, giving mirror-imaged CD curves with a positive first Cotton effect around 450 nm for the faster enantiomer and a negative one for the slower enantiomer. Because of the identity of the two porphyrin chromophores of **4a**, a first assignment of the enantiomers was achieved by applying the exciton chirality approach.<sup>26</sup> Accordingly, the corresponding faster eluting atropo-enantiomer (peak A) was attributed the *P*-configuration, and the more slowly eluting one (peak B) should be *M*-configured.<sup>29</sup>

This empirical result was further corroborated by quantum chemical CD calculations.<sup>30–32</sup> Starting with (*M*)-**3a**,<sup>33</sup> the conformational space was investigated by means of the PM3<sup>34</sup> method, resulting in 32 minimum geometries, which differed only in the dihedral angles of the peripheral phenyl substituents.

Because these groups should not significantly influence the molecular CD,<sup>35</sup> only the global minimum structure was

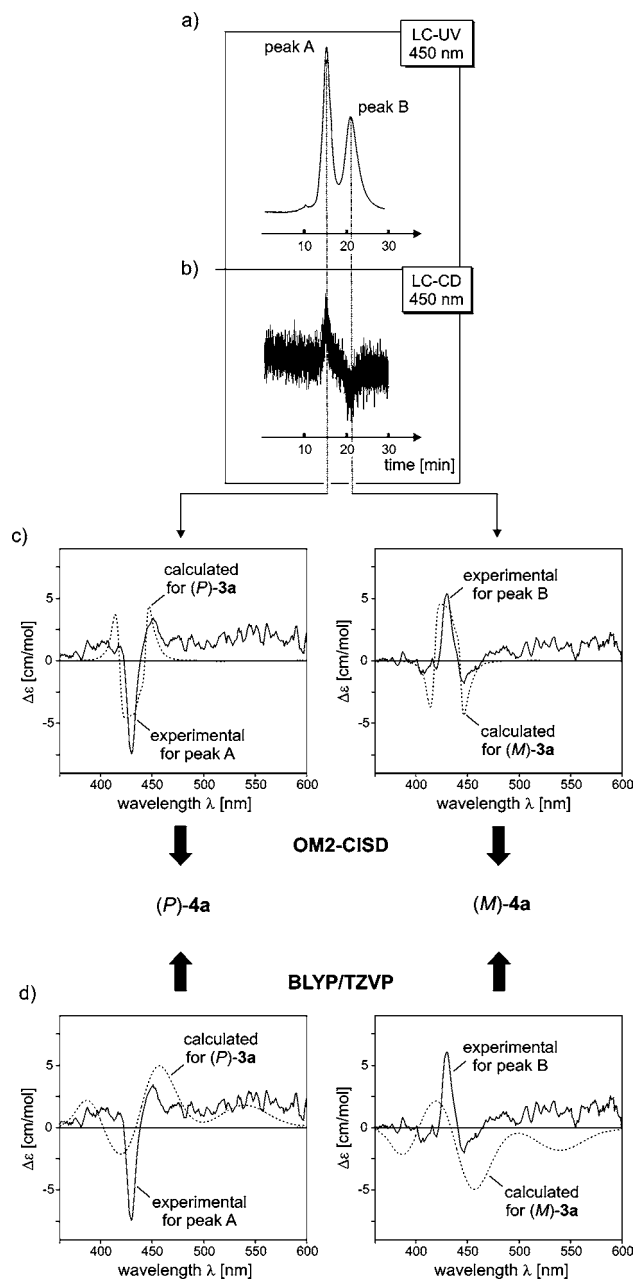


**Figure 2.** Stereochemical assignment of the two atropo-enantiomers of **4a**, by LC–CD coupling (separation on a Chiralcel OD-H column) and quantum chemical CD calculations for **3a**.<sup>33</sup>

further optimized using DFT (B3LYP/3-21G).<sup>36–38</sup> In this global minimum structure (Figure 3), the large porphyrin planes are near-orthogonal to each other (dihedral angle C-2–C-3–C-3′–C-2′ = 95°), whereas the phenyl substituents close to that axis (i.e., at C-5 and C-5′) are, in turn, orthogonal to the corresponding porphyrin (with dihedral angles of 88° and 89°, respectively). The minimum structure likewise rationalizes the unsymmetric environment of the

(27) An identical chiral phase had been used previously for the separation of *meso*–*meso*-linked zincated porphyrin dimers.<sup>12</sup>

(28) Further chromatographic details: using a Chiralcel OD-H column (Daicel), 7 °C, a flow rate of 0.3 mL/min, and *n*-hexane/2-propanol = 60:40 as the eluent, or even more efficiently in the case of **4b**, using a Chirex 3010 column (Phenomenex), 25 °C, a flow rate of 1 mL/min, and *n*-hexane/dichloromethane = 60:40 as the eluent.

(29) This chromatographic order is true for both chiral adsorbants used, Chiralcel OD-H (Daicel) and Chirex 3010 (Phenomenex).

(30) Bringmann, G.; Busemann, S. *Natural Product Analysis*; Schreiber, P., Herderich, M., Humpf, H. U., Schwab, W., Eds.; Vieweg: Wiesbaden, 1998; p 195.

(31) Bringmann, G.; Mühlbacher, J.; Reichert, M.; Dreyer, M.; Kolz, J.; Speicher, A. *J. Am. Chem. Soc.* **2004**, *126*, 9283.

(32) Bringmann, G.; Gulder, T.; Reichert, M.; Meyer, F. *Org. Lett.* **2006**, *8*, 1037.

(33) Because Zn is not parametrized in the program packages that were used for the semiempirical calculation of excited states, the metal-free analogue of **4a** was investigated instead. This approximation seemed justified because the presence or absence of Zn should not influence the shape of the CD curve substantially.

(34) Stewart, J. J. P. *J. Comput. Chem.* **1989**, *10*, 209.

(35) To verify this assumption, three additional PM3 minimum geometries were also optimized with B3LYP/3-21G providing CD spectra identical to the one of the global minimum.

(36) Becke, A. D. *J. Chem. Phys.* **1993**, *98*, 1372.

(37) Becke, A. D. *J. Chem. Phys.* **1993**, *98*, 5648.

(38) Lee, C.; Yang, W.; Parr, R. G. *Phys. Rev. B* **1988**, *37*, 785.

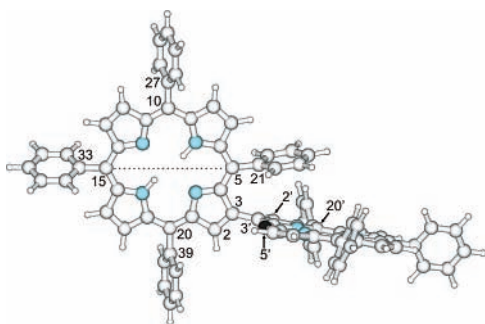


**Figure 3.** Calculated (B3LYP/3-21G) global minimum structure of **3a** (arbitrarily, only the P-enantiomer is shown). One phenyl substituent (at C-5', labeled in black) has been omitted for reasons of clarity; note the significant deviation at the phenyl groups at C-5 (in relation to the dotted line) in comparison to the unhindered other phenyl groups.

*ortho*- and *meta*-protons of the phenyl groups discussed above. The residue at C-5<sup>39</sup> is significantly bent away from the adjacent porphyrinyl substituent at C-3 as measurable by a deviation of 9° (angle of 171° for C-15–C-5–C-21 as compared to 180° for the undistorted cases C-27–C-10–C-20, C-10–C-20–C-39, and C-33–C-15–C-5); this is apparently a compromise between steric repulsion (of the phenyl substituent at C-5 and the one at C-20') and attractive interactions ( $\pi$ – $\pi$  stacking). The minimum structure also explains the observed largely different chemical shifts, e.g., of the *ortho*-protons of the phenyl substituent at C-5 in the <sup>1</sup>H NMR spectrum of **3a** (see above).

The minimum structure was then submitted to CD calculations by means of the OM2<sup>40</sup> Hamiltonian and TDDFT (BLYP<sup>38,41</sup>/TZVP<sup>42</sup>). The simulated CD curves thus obtained were both UV corrected<sup>30</sup> and compared with the experimental spectra of the faster (peak A) and the more slowly eluting (peak B) atropo-enantiomers of **4a**. The comparison revealed good agreements between (*P*)-**3a** and peak A (Figure 2c and 2d, left) and between (*M*)-**3a** and peak B (Figure 2c and 2d, right), thus permitting the absolute configurations to be assigned to the respective atropo-enantiomers, in full accordance with the above predictions of the exciton chirality method.

The difficult resolution of the two enantiomers of the zincated bisporphyrin **4a** and the failure for the metal-free

(39) Because of the C<sub>2</sub>-symmetry, the same applies for the phenyl group at C-5' (which, in turn, is bent away from the porphyrin substituent at C-3').

(40) Weber, W.; Thiel, W. *Theor. Chem. Acc.* **2000**, *103*, 495.

(41) Becke, A. D. *Phys. Rev. A* **1988**, *38*, 3098.

(42) Schäfer, A.; Huber, C.; Ahlrichs, R. *J. Chem. Phys.* **1994**, *100*, 5829.

parent compound **3a** suggested preparation of a related bisporphyrin with a higher rotational barrier at the axis—after all, **3** and **4** are heterobiaryls with only two substituents next to the central linkage. One option would be the—synthetically more challenging—possibility to fully block the rotation by an additional  $\beta$ -substituent at C-2, on the same pyrrole ring, which would increase the number of direct substituents next to the axis up to four. Molecular considerations, however, suggested that even *para*-methyl groups in the *meso*-phenyl rings of **3** or **4** might enhance the rotational barrier significantly, making the likewise novel bis(tetratolylporphyrin) **3b** an attractive—and certainly more easily attainable—target molecule.

The new porphyrin dimer **3b** was prepared following the methods elaborated above (cf. Scheme 1). A first experimental hint at a generally more fixed conformation in **3b** was the even stronger diastereotopic differentiation of the *ortho*- (7.12 and 5.90 ppm) and *meta*-protons (6.01 and 3.21 ppm) of the tolyl substituents in <sup>1</sup>H NMR as compared to that in **3a** and **4a** (see above). Under the chromatographical conditions elaborated for **4a**, however, again only the metalated  $\beta,\beta$ -bisporphyrin **4b** could be resolved, giving no indication of a significantly increased configurational stability at the axis. Quantum chemical calculations (AM1) delivered a comparably low rotational barrier  $\Delta G^\ddagger$  for the tolyl derivative of 94 kJ/mol in **3b** (and of 119 kJ/mol for the zinc complex **4b**) as compared to 110 kJ/mol for the bis-(tetraphenylporphyrin) **3a** (and 115 kJ/mol for its zincated analogue **4a**).

This very first synthetic access to rotationally hindered axially chiral directly  $\beta,\beta$ -linked bisporphyrins makes the design and preparation of further such “extended biaryls”, the exploration of their structural, spectroscopic, and optical properties, and their utilization a rewarding task. This work is in progress.

**Acknowledgment.** This work is dedicated to Professor Siegfried Hünig on the occasion of his 85th birthday and was funded by the Fonds der Chemischen Industrie. The authors gratefully acknowledge Dr. habil. Teodor S. Balaban and Dipl. Chem. Viviana Lorelei Horhoiu, DFG Centre for Functional Nanostructures, University of Karlsruhe, Germany, for a generous first gift of **1a**.

**Supporting Information Available:** Experimental procedures and NMR spectra for obtained compounds. This material is available free of charge via the Internet at <http://pubs.acs.org>.

OL061812O